

DEVELOPMENT OF IMPROVED EXTERNALLY PRESSURIZED GAS BEARINGS

R. Snoeys* and F. Al-Bender*

(Received April 10, 1987)

As a result of recent research and development work at the K.U.Leuven(Belgium), a number of airbearings with non-parallel airgaps have been designed for which some disadvantages(high costs, low load carrying capacity, small bearing stiffness and sensitivity to pneumatic hammering) have been eliminated or strongly attenuated. The conically shaped airgaps yield a larger thrust force and an increased bearing stiffness.

The dynamic behaviour of the air film may be fully characterized as a function of bearing parameters, enabling one to predict the stability limits for a particular application.

Key Words : Air Bearing, Air Film, Bearing Stiffness, Stability

NOMENCLATURE

A	: Bearing area(m ²)
a _m	: Membrane thickness(m)
C	: Friction moment(Nm)
d	: Spindle diameter(m)
F	: Bearing force(N)
ΔF_r	: Dynamic load generated in gas film(N)
$F_{\max} = Ap_s$: Maximum theoretical load capacity(N)
h	: Overall bearing displacement(m)
Δh	: Gap width variation(m)
h _b	: Height of bump on the mating bearing surface(m)
h ₀	: Gap at outside radius(m)
h ₁	: Gap at inside radius(m)
$h_v = h_1 - h_0$: Gap difference(m)
I _c	: Critical diametral moment of inertia(kgm ²)
K _r	: Dynamic stiffness of gas film(N/m)
K	: Bearing stiffness of the compensated thrust bearing(N/m)
m _c	: Critical mass(kg)
p	: Pressure distribution in gap(Pa)
p _a	: Atmospheric pressure(Pa)
p _g	: Preload pressure(Pa)
p _s	: Supply pressure(Pa)
p _v	: Pressure at the gap entrance(Pa)
Q	: Mass flow(kg/s)
ΔR	: Difference of spindle radius and nominal pad radius(m)
r	: Radius(m)
r ₀	: Outer radius(m)
r ₁	: Inner radius(m)
r _b	: Radius of bump on mating bearing surface(m)
θ	: Half pad angle(rad)
μ_r	: Coefficient of friction(-)
w	: Angular frequency(rad)

1. INTRODUCTION

Air-bearings in general and externally pressurized gas-bearings in particular require extremely high manufacturing accuracies. Moreover, bearing loads as well as obtainable stiffnesses are, usually, rather limited.

Cost of air-consumption and dynamic stability problems are often considered as important drawbacks.

*Katholieke Universiteit Leuven, Department Werktuigkunde Afdeling Mechanische Productie en Constructie, Celestijnenlaan 300B -3030, Heverlee, Belgie

At the K.U.Leuven a number of externally pressurized gas-bearings have been designed and tested for which those often mentioned disadvantages are eliminated or, at least, strongly attenuated.

The field of application of suchlike bearing types may therefore be considerably enlarged.

The main features of gas-bearings may be recalled :

- Low frictional losses
- Large temperature application range
- Wide speed range
- Negligible wear
- High rotational precision
- Low level of bearing noise
- Use of process fluidum as lubricant
- Reduced danger of contamination

Some possible fields of application for externally pressurized gas-bearings are therefore :

Machine construction(grinding and drilling spindles-slide ways of NC-machines-index tables-gyroscopes-turbines-air-and spacecrafts, etc.)

Metrology(reference spindles-3D measuring machines-etc.)

Data retrieval systems(transport of mag tapes-support of magnetic reading heads, disc supports, etc.)

Particular features of newly designed bearings

(1) Reduced cost

The manufacturing cost may be reduced significantly as a result of the use of some high accuracy epoxy castings technique, and of the larger tolerance allowances of spindle and bearing dimensions. Maintenance costs may also be kept small when the bearing system consists of easily mountable and replaceable standard elements.

(2) Low level air-consumption

The flow rate may be reduced by some 200% using convergent bearing gaps instead of parallel ones.

(3) Improved carrying capacity and stiffness values

The maximum load of those bearings may be 300 to 500% larger than that of the "classic" ones, because the major part of the total pressure drop occurs in the bearing gap(and not in the restrictor). The stiffness may be increased to any desired value when some stiffness compensation technique is applied(Blondeel et al., 1976a).

(4) Improved reliability

Large feed hole diameter may be used which are less prone to blockage by dust particles.

Self-aligning pads compensate easily for any mounting errors.

(5) Improved stability

Problems of dynamic instability(pneumatic hammering)

can be systematically predicted and avoided.

2. DESIGN PRINCIPLES

2.1 Gap Geometry as Control Element

The load capacity as well as the stiffness value of externally pressurized bearings may be substantially improved by using the bearing gap geometry as a controlling element in a servo loop.

Moreover the bearing surface itself can be designed to deflect in such a way as to create a new gap geometry and consequently another pressure distribution, compensating thereby for the change of external load variations.

Even a bearing with an infinite stiffness may be obtained, provided that the built-in system has a "negative" stiffness of exactly the same magnitude as the stiffness of the bearing gap (Blondeel et al., 1976a). The adjective "negative" means that force and deflection have opposite directions.

The main design principles with variable gap geometry are :

The control function of the restrictor is assigned partially or completely to the gap itself. As a result, the pressure drop in the restrictor is reduced, and higher pressures are available in the gap, leading to an increased load capacity.

A large load capacity, and especially, a high bearing stiffness, are obtained when the convergence of the gap in the flow direction is made to become an increasing function of the external load.

A cross section of an air-bearing pad is represented in Fig. 1. The type represented is one with a variable gap geometry, obtained by a membrane deflected by the difference of the pressure acting on its upper and lower sides.

In case of equal pressures on both sides of the membrane, no elastic deformation of the latter occurs, it remains in its original (conical) position. Such a situation arises when the load on the the bearing is so large that the outer rim of the bearing touches the opposite bearing surface(Fig.1a).

In that case the pressures on both sides of the membrane are the same.

When the external load F decreases, the mass flow Q through the gap increases because of the larger gap width. As a result, the pressure drop in the central restrictor or inlet area increases as well.

Consequently, the pressure p_v at the gap entrance, in its turn, decreases. As indicated in Fig.1b, the pressure in the gap

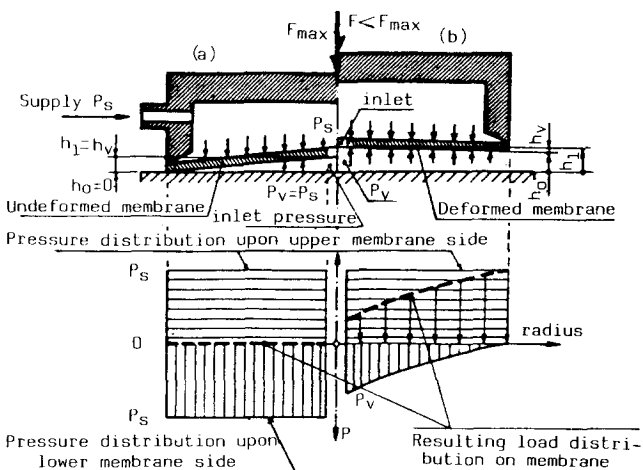


Fig. 1 Thrust bearing with variable gap geometry.

will drop gradually from the maximum value p_v in the centre to the atmospheric pressure (p_a) at the outer rim, resulting in a less conical gap shape.

The change of the pressure distribution in the bearing gap will balance the decrease of the external load.

2.2 Control of Thrust Force by Shape Pressure Distribution

The control function of the restrictor may also be assigned to a non-compliant bearing surface with a constant convergent gap shape(Fig.2). In contrast with a parallel gap, the shape of the pressure distribution in a convergent gap depends on the actual value of the gap width(Fig.3). A change of the gap magnitude creates a variation of the pressure distribution function. This in turn yields a variation of the load carrying capacity of the bearing and is, indeed, the negative feedback to the initial cause of the gap width change.

Both of the above mentioned design principles lead to performance characteristics superior to those of parallel gap bearings(see section 3.1 below).

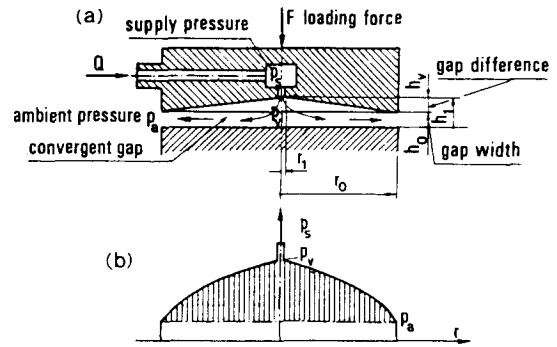


Fig. 2 Thrust bearing with fixed convergent gap.

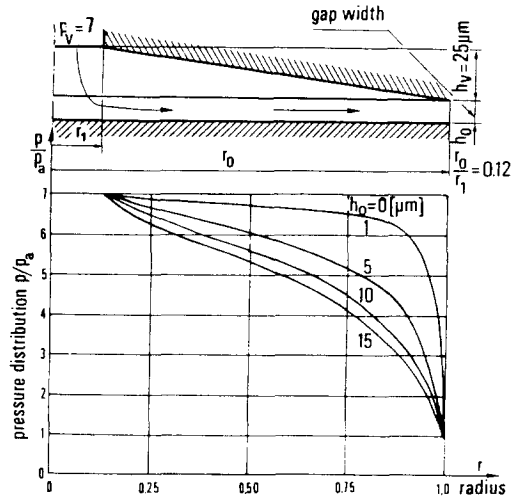


Fig. 3 Pressure distribution in convergent gaps as a function of gap width h_0 .

2.3 Bearings with Stiffness Compensation

(1) Working principles

When bearings with load-depending conicity are used, any change of the gap geometry creates a new pressure distribution in the bearing gap, insuring the equilibrium of action(load) and reaction(resultant force of pressure).

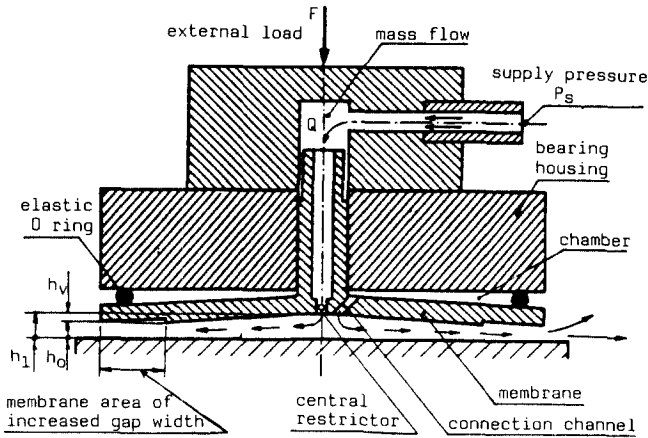


Fig. 4 Thrust bearing with centrally supported membrane.

The required variation of the gap geometry is obtained either by a relative rigid body motion of both bearing parts, or by a deflection of a deformable bearing surface. If the deformation of bearing surface is relatively large, the additionally required rigid body motion is decreased.

This feature is called a stiffness compensation because this arrangement may increase significantly the overall bearing stiffness.

The rigid body motion or bearing displacement may be eliminated completely if the change of the gap geometry associated with the elastic deflection of the bearing surface sufficiently influences the pressure distribution in the gap. Such a situation corresponds with an infinitely stiff bearing system. An over-compensation in this respect (obtained by adapting the membrane area of increased gap width—Fig.4) even yields a bearing with “negative” stiffness (Blondeel et al., 1976a).

A special design for an axial bearing is schematically shown in Fig.4. One of the bearing surfaces is now a centrally supported membrane. The chamber between the membrane and the bearing house is sealed by a compliant gasket. The chamber located above the membrane, is maintained at the pressure of the gap entrance by means of a connection channel.

(2) Characteristics of compensated bearings

As indicated in Fig.4, the overall bearing displacement is

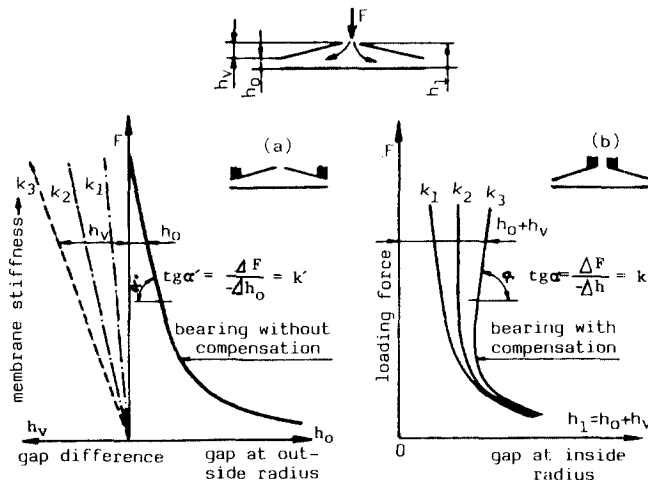


Fig. 5 Influence of support location on the overall bearing characteristic (Qualitative assessment of the influence of membrane stiffness.)

equal to the variation of the bearing gap h_1 at the centre. This particular value of the gap may be split up into the bearing gap at the outer rim h_0 and the gap difference h_v (Fig. 5a). The load-displacement characteristic ($F-h_1$) of the compensated bearing can be found from the combination of both functions (h_v-F ; h_0-F). This is illustrated by Fig.5b for different stiffnesses of the membrane. The slope of the characteristic curve associated with the stiffness k_3 indicates that a “negative” stiffness is obtained; an increase of the load yields a larger gap h_1 . For a compensated bearing the overall bearing stiffness is :

$$k = \frac{dF}{d(h_0+h_v)} = - \frac{\Delta F}{\Delta h_0+h_v}$$

The gap variations h_0 and h_v always have opposite signs for a centrally supported membrane (Fig.4).

An infinite stiffness k may be obtained if :

$$|h_0| = |h_v|$$

A relatively small membrane stiffness yields a negative overall bearing stiffness. this type of bearings may be optimally designed, with the aid of simple design charts, to give infinite stiffness over 20% of the bearing load range (Byant et al., 1986). No pneumatic instability will occur as long as the gap difference h_v does not become excessively large.

(3) Experimental results

A bearing as shown in Fig.4 was built, with functional dimensions as indicated in Fig.6. The load-displacement characteristics of this compensated bearing for different supply pressures is shown. With a supply pressure of 0.2 M Pa the bearing always shows a positive stiffness.

When supplied with a pressure of 0.26 M Pa a relatively large load range is obtained with an infinite bearing stiffness. For higher supply pressures, The bearing is over-compensated and shows a range of negative stiffness.

It is obvious that this kind of bearing design is quite interesting as it offers unique stiffness characteristics. The gas consumption remains small as can be expected from the use of variable gap geometry. The same technique can also be applied for radial bearings.

In order to verify the pressure distribution experimentally, a test rig was designed and built as shown in Fig.7.

The pressure distribution ($p=f(r)$) measured by means of this set-up for a parallel bearing gap is shown in Fig.8. The results refer to various loads applied on the axial bearing

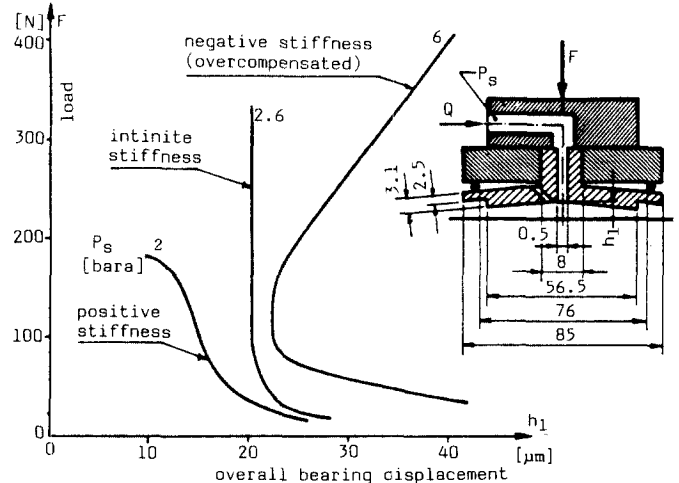


Fig. 6 Experimental characteristics of compensated bearing.

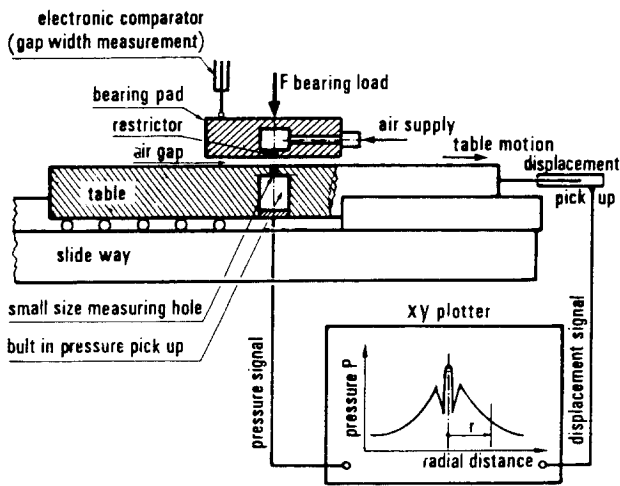


Fig. 7 Test rig for pressure distribution measurement.

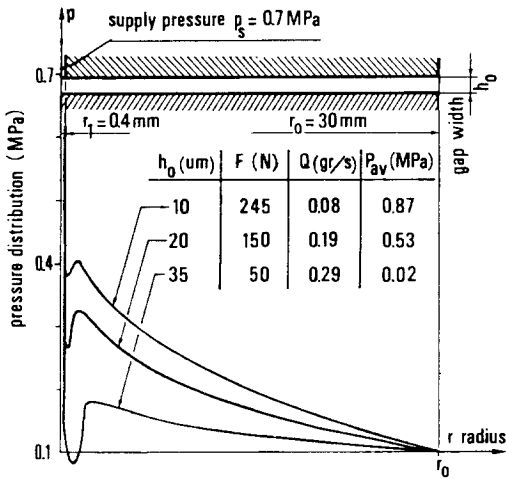


Fig. 8 Experimentally determined pressure distributions for a bearing with parallel gap.

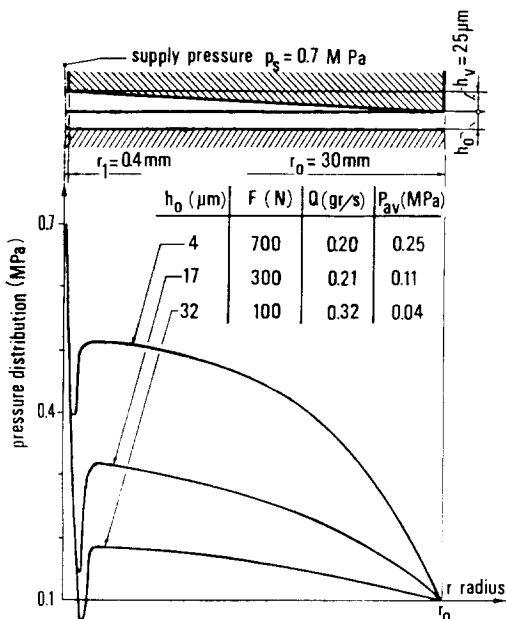


Fig. 9 Experimentally determined pressure distributions for a bearing with convergent gap.

pad associated with a particular magnitude of the gap width. In the same figure, values of flow rate are also indicated.

The pressure distribution function in the vicinity of the restrictor shows some kind of discontinuous pressure variation; this is due to the turbulent nature of the flow at the gap entrance (Mori and Ezuka, 1975). The experimental results for bearing geometries with a convergent bearing gap are summarized in Fig.9 (gap difference $h_v = 25 \mu\text{m}$).

A much more favourable pressure distribution is obtained yielding larger thrust forces. The shape of the pressure distribution function changes substantially when the load increases (or the gap width decreases). This phenomenon constitutes a feedback mechanism eliminating partly or completely the need for a restrictor even for noncompliant types of bearing surfaces. Consequently, a more effective use of the total available pressure drop can be expected.

3. BEARING CHARACTERISTICS

3.1 Load and Mass Flow Characteristics

The load and the mass flow are plotted versus the nominal bearing gap (Figs.10 and 11).

Three different (radial) pad types are compared:

- parallel gap
- fixed convergent gap
- variable gap

In the plot (Fig.10) load characteristic of a bearing pad with a variable gap geometry is superimposed with those obtained from a bearing gap with parallel gap and a pad having a fixed convergency. The slope at small values of the bearing gap (h_0) is of special concern.

The influence of variable gap geometries in terms of mass flow is shown in Fig.11. They lead to a smaller air consumption

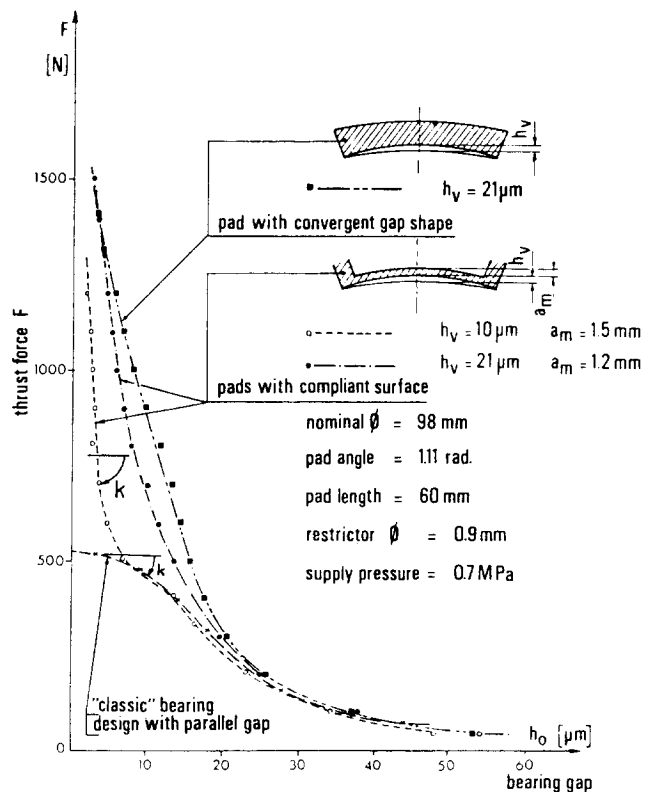


Fig. 10 Force displacement characteristics of bearings with parallel, convergent and compliant bearings surface.

Table 1 Comparison of bearing pads with different gap geometries.

Gap type	Gap width μm	Stiffness		Load		Flow rate gr/s
		$\frac{\text{N}}{\mu\text{m}}$	$\frac{10^{-3}\text{N}/\mu\text{m}}{\text{m}^2 \cdot \text{p}_a}$	N	$\frac{\text{N}}{\text{m}^2 \cdot \text{p}_a}$	
Parallel	10	16.6	9.0	460	0.25	0.32
	5	4.6	2.5	510	0.28	0.18
Convergent $h_v = 21\mu\text{m}$	10	64.4	35.1	870	0.47	0.45
	5	77	42.0	1240	0.768	0.27
Compliant $h_v = 21\mu\text{m}$	10	52.2	28.4	670	0.36	0.42
	5	130	70.8	1130	0.62	0.27

The result of this theoretical approach is given in Fig.12a and b. Bearings with parallel gaps below $20\ \mu\text{m}$ turn out to be statically unstable even for small size irregularities ($h_b = 2.5\ \mu\text{m}$).

This is illustrated in Fig.12a where, in some cases, the stiffness of the bearing (slope of force displacement curve) changes its sign with the gap width.

The force-displacement characteristics for convergent gap bearings, on the other hand, do not show any region of negative stiffnesses for irregularities remaining smaller than the gap difference h_v . The passage of this kind of irregularity results, in this case, merely in some relatively small change in the gap width.

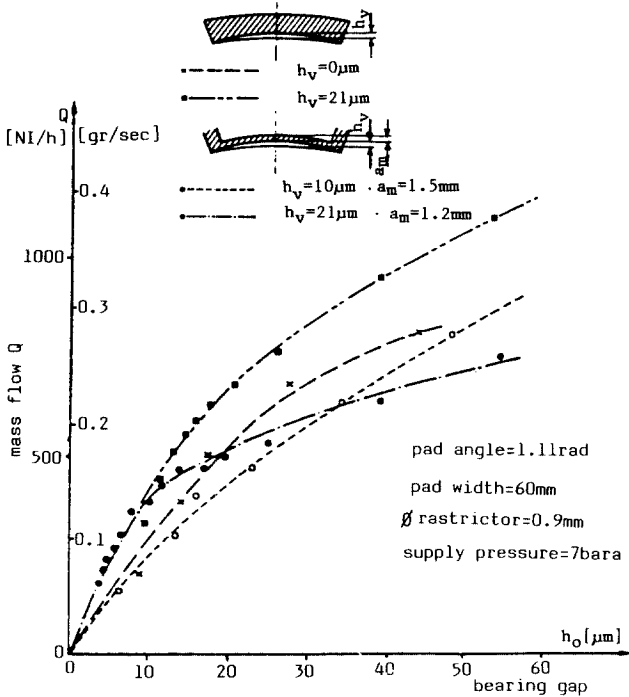


Fig. 11 Comparison of mass flow versus nominal bearing gap for different pad types.

tion for relatively large gap widths. The stiffness, load capacity and gas flow are compared in Table 1 (nominal diameter = 98 mm, pad angle = 1.11 rad, pad width = 60 mm, diameter restrictor = 0.9 mm, supply pressure = 0.7 MPa).

3.2 Influence of Bearing Surface Irregularities

Bearings with parallel gaps are quite sensitive to irregularities (scratches, bumps, etc.) of the moving bearing surface. It was experimentally found that the pressure distribution function remains almost undisturbed as long as the "bump" stays outside the "area of influence" of the feed hole. The gap width remains unchanged as well.

However, as soon as the bearing surface irregularity or "bump" reaches the restrictor area, an instant drop of the load carrying capacity occurs, yielding a sudden mechanical contact of both bearing surfaces.

Bearings with convergent gap geometries are far less sensitive to this disturbing phenomenon. To quantify the sensitivity of various bearing geometries with respect to bearing surface irregularities, two particular types of irregularity have been selected as shown in Fig.12. Using a model insuring viscous gas flow and neglecting throttling at the entrance, the load force is evaluated for various gap widths h_o as well as for a set of different heights of the bumps h_b .

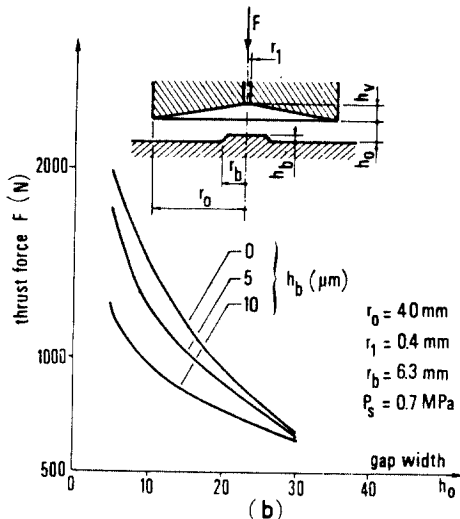
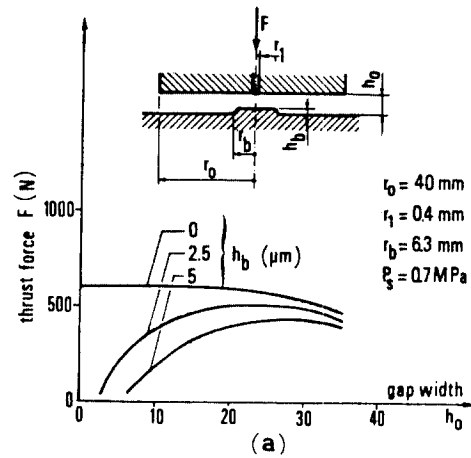


Fig. 12 Theoretically determined influence of bearing surface irregularity for : a) parallel bearing ; b) convergent bearing.

3.3 Sensitivity to Tolerance Deviations

To evaluate the influence of shaft/bearing tolerances, a number of bearing characteristics have been measured for various spindle-bearing combinations (shaft diameter difference from +0.5 to -0.5 mm with respect to the nominal diameter of the bearing gap). Some results of those investigations are summarized in Fig.13 for three different pad types. In this figure the specific load (load/active bearing surface) and mass flow associated with a bearing gap of 10 μm are plotted versus the difference between shaft diameter and nominal diameter.

Pads with a convergent gap turn out to be considerably less critical to shaft tolerance deviations compared to pads with parallel gaps. To obtain the same thrust force as for a bearing with parallel gap and nominal diameter, a difference of even 0.5mm can be tolerated. The shaft diameter may be slightly (100–150 μm) smaller than the nominal pad diameter; this would result in a somewhat smaller air consumption without changing too much the load-carrying capacity.

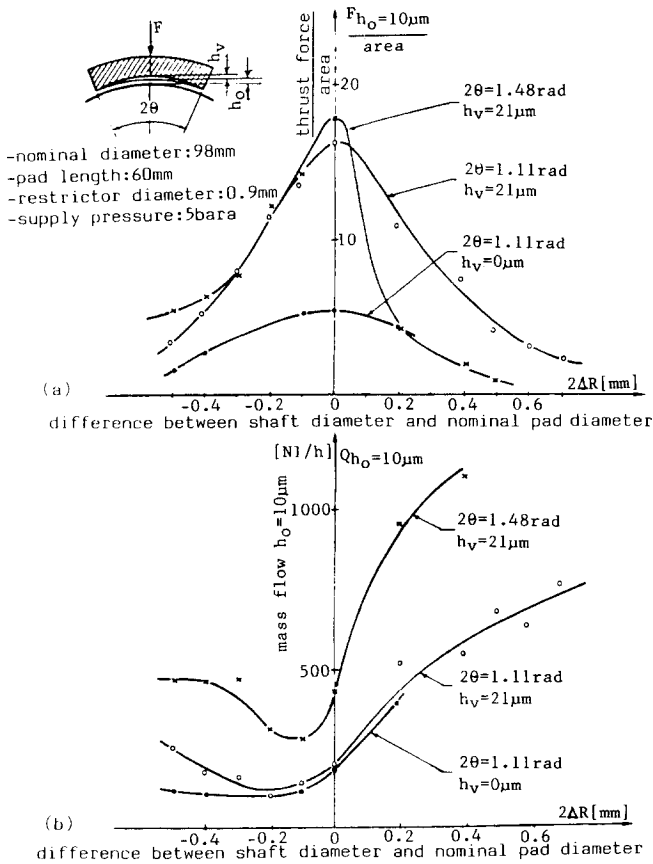


Fig. 13 Thrust force and mass flow versus difference between shaft diameter and nominal pad diameter, for an air gap $h_0=10\mu\text{m}$.

3.4 Frictional Characteristics of Air Bearings

Friction forces were determined at various low rotational speeds of spindles mounted on radial air bearing pads.

The friction moment increases linearly with the rotational speed (March, 1976). Typical results, expressed as coefficient of friction μ_t with respect to the relative sliding speed of the bearing surface, were; $\mu_t=45 \times 10^{-6}$ at speed of 1m/s, increasing at the rate of 36×10^{-6} m/s.

4. DYNAMIC STABILITY OF BEARINGS

Pneumatic hammering is a kind of self-excited vibration generated in the bearing gap due to the compressibility of the gaseous lubricant.

4.1 Dynamic Identification of the Bearing Film

The dynamic behaviour of the air gap was investigated theoretically and experimentally by considering the frequency response function (F.R.F.) of the air film as a mechanical component. This F.R.F. is expressed as the dynamic stiffness $K_t(w)$ of the air film :

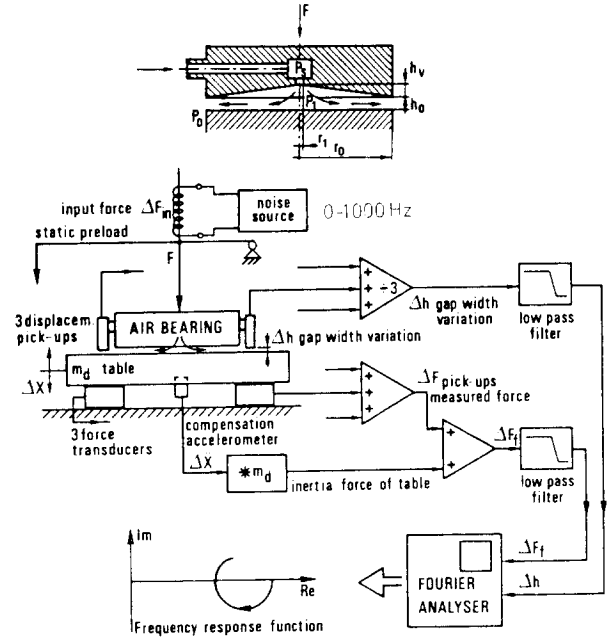


Fig. 14 Test set-up for determination of F.R.F. of air film.

Table 2 Influence of the bearing parameters on the frequency-response function of the gas film.

Parameter	Symbol	Film stiffness (real part of K_t)	Damping value (imag. part of K_t/w)
Supply pressure	p_s	↗	↘
Gap difference	h_v	↗	↘
Outer diameter	d_o	↗	↘
Gap width	h_0	↘	↘
Diameter of feed-hole	d_1	→	↗

dynamic stiffness $K_t(w)$ of the air film :

$$K_t(w) = \frac{\Delta F_t(w)}{\Delta h}$$

Theoretically, $K_t(w)$ was determined by solving the time dependent Reynold's equation for a fixed conical gap geometry, by a predictor-corrector method.

The results obtained from the theoretical model were experimentally verified by means of a test set-up as shown in Fig.14. Figure 15 shows a good agreement between the two (Plessers and Snoeys, 1985b).

Since the stability of air bearing performance is dependent on this F.R.F. (the imaginary part of which representing the damping), the influence of the basic bearing parameters on it was investigated with the aid of the theoretical model. The general results of this investigation are presented in Table 2

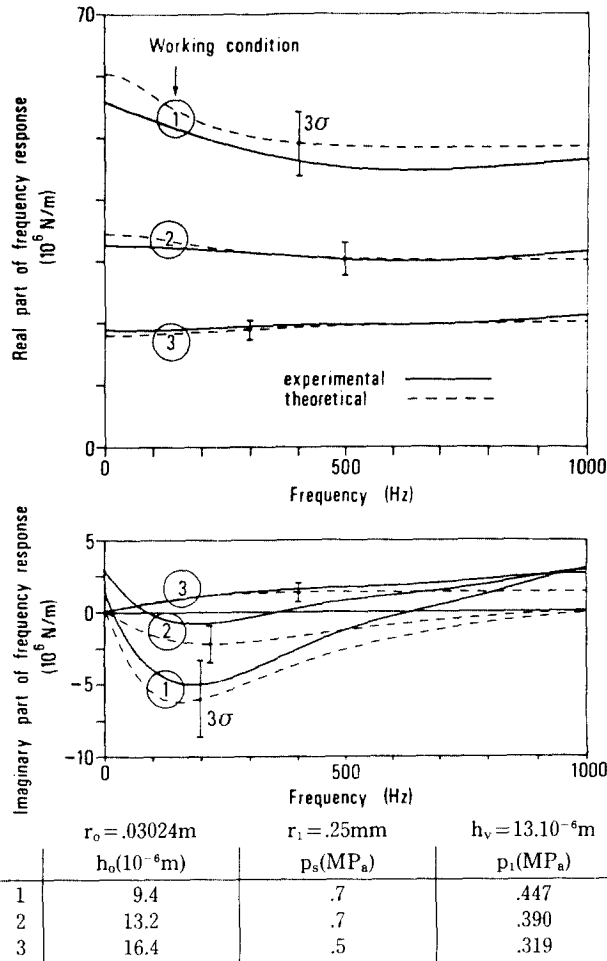


Fig. 15 Comparison between measured & calculated freq. Response function of an air gap.

(Plessers and Snoeys, 1985b).

Some recent research shows that it is possible to improve the efficiency and accuracy of the theoretical model, yielding useful design guidelines for unconditionally stable bearings.

4.2 Air Bearings in Mechanical Systems

Based on the now readily available dynamic characteristics of the air film, stability criteria for mechanical systems containing more than one air bearing could be worked out systematically using the Nyquist criterion. This resulted in some rules of thumb which may be quite useful for the design of bearing systems (Plessers and Snoeys, 1985b) : pneumatic hammering may be eliminated by a proper selection of bearing and/or structure parameters.

As an example, a test was carried out in which a rigid disc was mounted on three aerostatic pads as shown in Fig.16, being loaded on top by three identical masses placed symmetrically around its central vertical axis.

Thus, by shifting these masses away from the centre, the total mass remains the same while the moments of inertia are changed. The dynamic characteristics of the air gaps, and of the system as a whole, had been predetermined. From those, a critical mass m_c and a critical(diametral) moment of inertia I_c were established (exceeding which the system should be unstable in the translation and tilt modes, respectively). The test showed that there was no instability in the axial direction, since the mass was well below m_c , but that tilt vibrations would commence as soon as the diametral

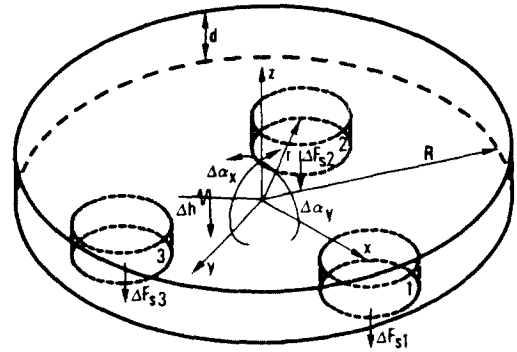


Fig. 16 Geometry of circular disc supported on three bearing pads.

moment of inertia approached I_c ; the frequency of these vibration was very close to that which had been predicted theoretically.

In [Plessers, 1985,(pp.6~43)], a scheme is suggested to control the stability of aerostatic bearings in mechanical structures.

4.3 Aerodynamic Effects

It is often desirable to use aerostatic bearings in a wide speed range. The aerostatic assumption for bearing design remains valid when the relative sliding speed of the two bearing surfaces is small in comparison with the average speed of air through the gap (50 m/s). When this is not so, however, a significant aerodynamic effect is introduced, affecting the bearing performance characteristics. Work is being carried out to investigate this aspect both theoretically and experimentally.

5. MANUFACTURING TECHNIQUES

Some rather simple and consequently cheap construction techniques may be applied to obtain the desired convergent bearing gaps.

5.1 Compliant Bearing Surfaces

Pads with a compliant bearing surface of a desired conicity may be obtained by deflecting the membrane(with the pressure of a fluidum or with a screw). In this deformed situation, a machining operation(Fig.17) or some kind of epoxy casting operation(Fig.18) produces again a perfect flat membrane surface. When reducing the applied pressure(or the force applied with a screw) the membrane will elastically deflect back to its original unloaded position creating the conical shape of the bearing surface.

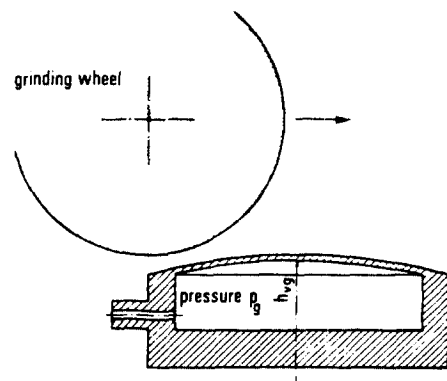


Fig. 17 Surface grinding of conical membrane.

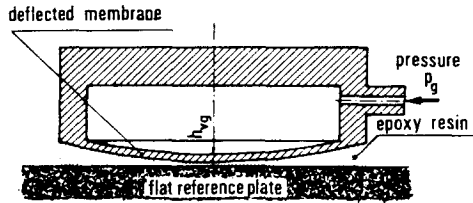


Fig. 18 Shaping of conical membrane by epoxy casting operation.

5.2 Non-Deformable Bearing Surfaces

Bearing pads with a non-deformable wall may be manufactured with a similar casting technique as indicated in Fig.18; however, the casting has to be carried out now with respect to an appropriate negative shape. This casting model for a radial bearing pad may be obtained as illustrated in Fig.19. The molding cylinder is provided with a membrane.

Cylinder and membrane are accurately machined at the nominal diameter of the bearing pad. The membrane may be deflected radially corresponding to the desired amount of the convergency of the gap. The same technique can be used for axial bearing pads, the bearing pad itself may also be made directly by diamond-tool turning on a precision lathe.

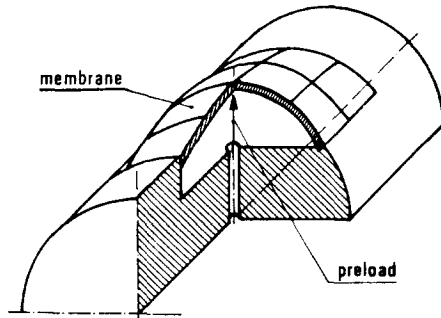


Fig. 19 Negative casting mold for radial bearing pad.

6. CONCLUSIONS

(1) A significantly larger carrying capacity may be obtained by using convergent gap shapes. The resulting bearing stiffness is increased, the airconsumption is reduced and problems of static stability are eliminated.

(2) Deformable bearing surfaces yield quite some interesting bearing load characteristics, to the point of obtaining infinite or negative bearing stiffness.

(3) Bearings with convergent gaps are considerably less affected by bearing surfaces irregularities. Very low friction in air-bearings still remains, of course, an important advantage in comparison with other bearing types.

(4) The above mentioned bearings show better static

stability. Their dynamic instability in mechanical systems may be accurately predicted and avoided by a proper selection of working and design parameters.

(5) The bearing geometry necessary to obtain optimum bearing characteristics can easily and cheaply be manufactured by a surface grinding operation or an epoxy resin casting technique.

REFERENCES

- Blondeel, E., 1975, "Aërostatistische Lagers Met Lastafhankelijke Spleetconfiguratie", Ph.D. Thesis, K.U. Leuven.
- Blondeel, E., Snoeys, R., and Devrieze, L., 1976a, "Aerostatic Bearings with infinite Stiffness", Annals of the CIRP, Vol. 25/1.
- Blondeel, E., Snoeys, R., and Devrieze, L., 1976b, "Externally Pressurized Bearings with Variable Gap Geometries", 7th. International Gas Bearing Symposium, Cambridge, July 13-15.
- Blondeel E., Snoeys, R., and Devrieze, L., 1980, "Dynamic Stability of Esternally Pressurized Gas Bearings", ASME J. of Lubrication Technology, Vol. 102.
- Byant, M.R., Velinsky, S.A., Beachly, N.H., and Fronczak, F. J., 1986, "A Design Methodology for obtaining Infinite Stiffness in an Aerostatic Thrust Bearing", ASME J. of Mechanisms, Transmissions, and Automation in Design.
- Constrantinescu, V.N., 1959, "Gas Lubrication", The A.S. M.E.
- Devrieze, L. and Snoeys, R., 1978, "Low Cost Externally pressurized Air Bearings", Proceedings of the 19th. M.T.D.R. Conference, Manchester, UMIST, pp.97-105.
- Gross, W. A., 1962, "Gas Film Lubrication", Wiley, New york, London.
- Lowe, I.R.G., 1974, "Characteristics of Externally pressurized Thrust Bearing with One Compliant Surface", Paper A4, 6th international Gas Bearing Symposium, University of Southampton.
- March, H., 1976, "Design for Minimum Total Power", 7th. International Gas Bearing Symposium, July 13-15, Cambridge.
- Mori, H. and Ezuka, H., 1975, "A Pseudo Shock Theory of Pressure Depression in Externally Pressurized Circular Thrust Gas Bearing", International Lubrication Conference, Tokyo, Japan.
- Plessers, P. and Snoeys, R. 1985a, "Dynamic Identification of Convergent Externally Pressurized Gas-Bearing Gaps", Subj. for Publication in ASME J. Tribology 1985.
- Plessers, P. and Snoeys, R., 1985b, "Dynamic Stability of Mechanical Structures Containing Externally Pressurized Gas Lubricated Bearings", Subj. for Publication in ASME J. Tribology 1985.
- Plessers, P., 1985c, "Dynamische instabiliteit Van Aerostatische Gaslagers in Mechanische Systemen", Ph. D. Thesis, K.U.Leuven.
- Snoeys, R., Devrieze, L. and Vanherck, P., 1977, "Self Aligning Aerostatic Shoe Bearings", Annals of the CIRP. Vol. 25/1, pp.205-210.